

**FEDERAL UNIVERSITY OF SÃO CARLOS
CENTER FOR EXACT SCIENCE AND TECHNOLOGY
MATERIALS ENGINEERING DEPARTMENT**

**Friction Riveting of Printed Circuit Boards (P.C.B.) and
Aluminum Hybrid Joints: Joint Formation Analysis and
Characterization.**

Maria Clara Farah Antunes Vilas Bôas

São Carlos - S.P.

2022

Friction Riveting of Printed Circuit Boards (P.C.B.) and Aluminum Hybrid Joints: Joint Formation Analysis and Characterization.

A thesis presented to Material Engineering
Department to achieve a bachelor's degree
in Material Engineering

Supervisor: Piter Gargarella

Co-Supervisor: Lucian Blaga

São Carlos - S.P.

2022



ATA DE DEFESA DE TRABALHO DE CONCLUSÃO DE CURSO (TCC)

NOME: Maria Clara Farah Antunes Vilas Bôas

RA: 727405

TÍTULO: Friction riveting of printed circuit boards (PCB) and aluminum hybrid joints: joint formation analysis and characterization

ORIENTADOR(A): Prof. Dr. Piter Gargarella

CO-ORIENTADOR(A): Dr. Lucian Blaga

DATA/HORÁRIO: 14/04/2022, 10h

BANCA – NOTAS:

	Monografia	Defesa
Prof. Dr. Piter Gargarella	8	10
Profa. Dra. Lidiane Cristina Costa	8	10
Média	8	10

Certifico que a defesa de monografia de TCC realizou-se com a participação a distância dos membros Prof. Dr. Piter Gargarella e Profa. Dra. Lidiane Cristina Costa e depois das arguições e deliberações realizadas, os participantes à distância estão de acordo com as informações redigidas nesta ata de defesa.

Prof. Dr. Piter Gargarella

Inscription

I dedicate this work to my maternal grandparents, Badra and Rubens, with whom I will not be able to share this moment, but who encouraged me to chase my dreams throughout my childhood and youth and made me understand that I would only achieve them through studies.

ACKNOWLEDGEMENTS

The development of this bachelor thesis has valuable contributions of many people, who I sincerely would like to gratefully thank:

1. Professor Piter Gargarella, who since my second year in the university, gave me all the support and trust in my work, either in the research work in Brazil, Austria, or Germany.
2. Lucian Blaga and Camila Rodrigues, for the support, orientation, and friendship during the development of this work in the Brazilian-German binational cooperation program established between Hereon and UFSCar.
3. Dr. Jorge F. dos Santos and Prof. Dr. Benjamin Klusemann for the opportunity to develop this work in the Hereon Institute.
4. PANASONIC for sponsoring this project.
5. All the friends I made during the graduation, for the emotional support and the mutual contribution to the studies.
6. All the friends I made during my time in Germany, in special those who were with me daily for almost one and a half years, making me feel at home in another different country from my birthplace: Amanda, Mateus, Matteo, Tiago, Juliano, Jeronimo, Elaiza, Marta, Egnaldo, Halak, Riccardo, Camila, André, Ivan, Leire, Amaia, Nico, and Vasu.
7. All the Hereon community, who contributed to performing my experiments and my staying in Geesthacht. In special Menno, Angela and Dagmar.
8. My family, for all the support and the motivation to follow my dreams.
9. My friends from Santa Rosa de Viterbo, who followed my steps since school and always showed to be cheering for me.

ABSTRACT

This work addressed the feasibility study of the Friction Riveting joining process on glass-fiber-reinforced epoxy resin laminate sheet (FR4-PCB) and 2024-T351 aluminum alloy rivets by investigating the rivet scale effects, the amount of copper layer on the surfaces of the plates, and their influence on heat development, and material behavior as well as subsequent joint formation and properties, including microstructure and mechanical performance of the joints. The research work was carried out at the Institute of Materials Mechanics Solid State Joining Processes Helmholtz-Zentrum Hereon in Germany in collaboration with the Material Engineering Department of the Federal University of São Carlos. The one-factor-at-a-time (OFAT) approach was used to investigate the influence of process parameters on the process temperature, macro and microstructural deformation, and mechanical properties. The macro and microstructural characterization were carried out by light optical microscopy (L.O.M.) and the mechanical properties of the joints were determined by T-pull tensile testing. The results demonstrated the viability of the process for the case of FR4 material with AA2024; joints with good mechanical performance ($828 \text{ N} \pm 65 \text{ N}$) were achieved using FR4 composites plates with reduced thickness (1.5 – 3.0 mm), the thinnest plates successfully joined via Friction Riveting so far. The downscaling was accomplished regarding the size of the rivet and the joints made with a smaller diameter (4mm) rivet demonstrated similar results to the joints with a 5mm diameter rivet. To improve and analyze the main process parameters, the Design of Experiments (D.O.E.) was used. Considering the effect on the temperature generated during the process, the rotational speed shows a high impact, followed by the material combination (one or double copper layer), once the higher rotational speed generates greater friction between the metal and the composite and the high conductivity of the copper contributes to the heating spread.

RESUMO

Este trabalho aborda o estudo da viabilidade do processo de união por *Friction Riveting* em folha laminada de resina epóxi reforçada com fibra de vidro (FR4-PCB) e rebites de liga de alumínio 2024-T351, investigando os efeitos do tamanho do rebite, a quantidade de camada de cobre nas superfícies das placas e sua influência no desenvolvimento de calor e comportamento do material, bem como na formação e propriedades subsequentes da junta, incluindo microestrutura e desempenho mecânico. O trabalho de pesquisa foi realizado no *Institute of Materials Mechanics Solid State Joining Processes Helmholtz-Zentrum Hereon*, localizado na Alemanha, em colaboração com o Departamento de Engenharia de Materiais da Universidade Federal de São Carlos (DEMA). Para investigar a influência dos parâmetros na temperatura do processo, deformação macro e microestrutural, propriedades mecânicas, mecanismos de fratura e degradação térmica da zona de ancoragem das juntas, mudou-se um parâmetro por vez (método *one-factor-at-time*). A caracterização macro e microestrutural foi realizada por microscopia óptica (LOM) e as propriedades mecânicas das juntas foram determinadas por ensaios de tração em forma de *T-pull*. Os resultados demonstraram a viabilidade do processo para o caso do material FR4 com AA2024; juntas com bom desempenho mecânico ($828 \text{ N} \pm 65 \text{ N}$) foram alcançadas utilizando placas de compósitos FR4 com espessura reduzida (1,5 – 3,0 mm), as placas mais finas unidas com sucesso via *Friction Riveting* até o momento. O *downscaling* foi realizado em relação ao tamanho do rebite e as juntas obtidas com o rebite de menor diâmetro (4mm) apresentaram resultados parecidos com as produzidas com rivet de 5mm de diâmetro. Para melhorar e analisar os principais parâmetros do processo foi utilizado Design de Experimentos (DOE). Considerando o efeito na geração de temperatura durante o processo, a velocidade rotacional apresentou a maior influência, seguida da combinação de materiais (uma ou dupla camada de cobre), uma vez que a maior velocidade rotacional gera maior atrito entre o metal e o compósito e a alta condutividade do cobre contribui para a propagação do aquecimento.

FIGURES LIST

Figure 1: Press-fit fasteners representation [11]

Figure 2: Schematic description of the Direct Friction Riveting process: a) positioning of joining partners, b) rivet insertion into the polymer (friction phase), c) rivet plastic deformation (forging phase), and d) joint consolidation [12].

Figure 3: Schematic force-controlled FricRiveting diagram [12].

Figure 4: a) microstructure analysis and b) microhardness map of the AA 2024-T351 rivet in the extrusion direction.

Figure 5: Illustration of the aluminum rivets: A) 5 mm and B) 4 mm diameter.

Figure 6: FR4 plate and cross-sectional microscopy view from a) plates with two copper layers and b) single copper layer.

Figure 7: Automated RSM 410 welding system for the production of friction-riveted joints (image source: Hereon).

Figure 8: T-pull tensile testing holder adapter used to evaluate the tensile force properties in Friction Riveting.

Figure 9: OM micrographs of joint cross-sections produced with the joining conditions 1 and 2. H-values are related to the penetration depth and W-values to the deformation rivet tip of a) Condition 1 (unsuccessful) and b) Condition 2 (successful joint condition).

Figure 10: a) Infrared thermography of the process temperature development during Friction Riveting. b) Maximum average temperature (362 ± 7 °C) measured on the expelled thermoset flash material from three joints produced for Condition 2.

Figure 11: a) Microstructure features of a Friction-riveted PCB-FR4 single copper layer/AA-2024-T351 joint (Condition 2) and Vickers microhardness distribution of an AA 2024-T3 deformed rivet. b) Thermo-Mechanically Affected Zone of the metal, TMAZ, exhibits grain realignment in the direction of the material flow in the forged rivet tip c) Detail of the Heat Affected Zone of the metal, HAZ.

Figure 12: a) T-pull specimen before testing, b) cross-sectional view of failure through PCB plate, (c) lower and (d) upper FR4-PCB parts after T-pull testing.

Figura 13: Trials for 4mm rivet and FR4 joint – a) C3 (RS-7000 rpm; FF-4000 N; DaF-3 mm); b) C4 (RS-6000 rpm; FF-4000 N; DaF-3 mm); c) C5 (RS-5500 rpm; FF-4000 N; DaF-3 mm).

Figure 14: Pareto Chart obtained with temperature response from the combination of the parameters: rotational speed (parameter A), displacement of the spindle (parameter B), joining force (parameter C), and the material (parameter D).

Figure 15: (a) Surface plot and (b) contour plot of temperature in function of joining force (JF) and rotational speed (RS).

Figure 16: Contour plot of temperature for the parameters combination: a) DaF x RS, b) JF x RS and c) JF x DaF.

Figure 17: DOE graph with a surface response showing the influence on the ultimate tensile force (UTF) of each parameter analyzed and their combination.

TABLES LIST

Table 1 - AA 2024 chemical composition [16].....	7
Table 2 - Physical-chemical properties of FR4 material.....	9
Table 3 - Joints parameters for the first trials.	11
Table 4 - Design of Experiments (Box-Behnken surface designer) for the joints with 4 mm rivet. RS: rotational speed; DaF: displacement at friction; JF: joining force.	11
Table 5 - Geometrical features (W, H, and DP) of the friction-riveted joints and calculated volumetric ratio, VR.	17
Table 6 - Geometrical features (W, H, and DP) of the friction-riveted joints and calculated volumetric ratio, VR.	22
Table 7 - Tensile and temperature response from the DOE analysis.	23

SUMMARY

1. Introduction	1
2. Literature Review	3
2.1 Friction Riveting Technique	3
2.1.1 Principle of Process.....	3
2.1.2. Process Parameters	5
2.1.3. Recent studies about friction riveting.....	5
2.2 Joint Design Optimization	6
3. Materials and Methods	6
3.1. Materials	6
3.1.1. Aluminum Alloy 2024 – T351.....	6
3.1.2. Glass-Reinforced Epoxy Laminate Material (FR4).....	8
3.2. Methods.....	9
3.2.1. Joining Equipment and Procedure.....	9
3.2.2. Process Temperature Evolution, Microstructure, and Local Mechanical Properties..	14
3.2.3. Joint Formation Analysis	14
3.2.4. Local and Global Mechanical Performance	14
4 Results and Discussion	16
4.1. 5 mm rivet diameter	16
4.1.1. Joint Formation.....	16
4.1.2. Temperature evolution	18
4.1.3. Microstructural Analysis and Local Mechanical Performance.....	18
4.1.4. Global Mechanical Performance	19
4.2. 4 mm rivet diameter	20
4.2.1. Joint formation.....	20
4.2.2. Determination of process-properties-performance correlations and optimization approach via DOE.....	22
4.2.3. Effect of the Temperature	24
4.2.4. Effect of the Global Mechanical Properties	27
6. Conclusions	29

1. Introduction

The Friction Riveting (FricRiveting) technique was developed and patented in 2007 within the Helmholtz-Zentrum Geesthacht Centre for Materials and Coastal Research (HZG, now Helmholtz-Zentrum Hereon) [1]. The method is based on the principles of mechanical fastening and friction welding. One or more thermoplastics or composite components are joined with a cylindrical metallic rivet through frictional heating and pressure, where the former causes the rivet to plasticize and deform [2].

The feasibility of Friction Riveting has been demonstrated for a substantial number of material combinations. Studies have been conducted with hybrid friction-riveted joints of different aluminum alloys with unreinforced thermoplastics (Polyetherimide, PEI [3], and Polycarbonate, PC [4]). Additionally, the technique was also successfully applied in reinforced polymer, carbon, and fiberglass laminates (e.g., GF-PEI [5]; CF-PEEK [6], GF-PA6 [7], GF-P [8]) joined with titanium and aluminum rivets.

The present work will explore the Friction Riveting technique as an alternative for assembling components in printed circuit boards (PCBs) that support the electronic and mechanical assembly of electronic components.

The press-fit technology is a cold joining process, which consists of assembling a pin through a slightly smaller hole of the PCB plates, as demonstrated in Figure 1. The material's surfaces create a gas-tight connection so any molecule can fit between them, generating a solder with enough mechanical and very good electrical properties. Although the quality of the joint, the press-fit process has some limitations, such as the number of processing steps, the need for pre-drilled holes on both sides of the plate, the use of an anvil, and connecting/mating screws [10].

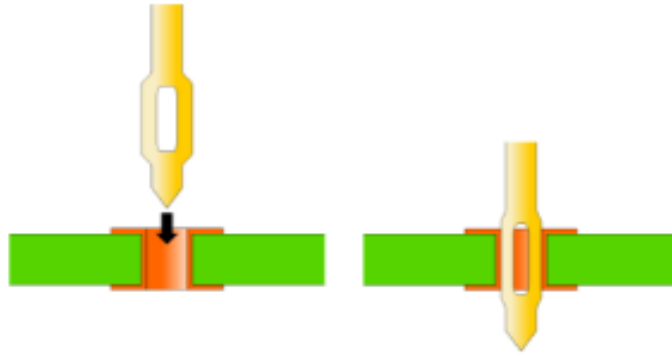


Figure 1: Press-fit fasteners representation [11]

This work aims to study the join formation feasibility using aluminum rivet and PCB materials spawned by the motivation to find feasible parameters for the Friction Riveting process as an alternative to the Press-Fit fasteners process printed on PCB. The main benefits of using Friction Riveting in PCBs are [2]:

1. The reduced number of process steps and short joining cycle;
2. No need for pre-drilling on both sides of the plate;
3. The fastener is directly anchored on the PCB through a single entrance;
4. No mating screw is required, leading to a decrease in component weight.

The present work studies the feasibility of the Friction Riveting technique and characterizes the obtained joints on glass-reinforced epoxy resin laminate sheets (FR4-PCB) and 2024-T351 aluminum alloy rivets by investigating their microstructure and mechanical properties.

2. Literature Review

2.1 Friction Riveting Technique

The Friction Riveting process is a new metal-polymer hybrid joining technology based on mechanical anchoring and rotational friction welding principles. The process involves a metallic rivet penetrating a polymer or composite plate due to the heat generated by the friction between the polymer and the rotating rivet [12]. Then, the rivet is deformed, anchoring inside the plate because of an axial pressure applied.

2.1.1 Principle of Process

The principles governing the manufacture of metallic-insert joints in thermoplastic are shown in Figure 2 in a simplified form, as follows: a) Positioning of joining partners: the rivet is first assembled on the chuck in the welding head and then, aligned with the plate in the place of the joint. b) Rivet insertion into the polymer (friction phase): a pre-set is done by touching the plate with the rivet. The spindle starts to rotate and an axial force is applied, heating the polymer around the rivet, which will plasticize and expel a flash from the joining area. Due to the heat generated at the tip of the rivet and the polymer's low thermal conductivity, the metal achieves the plasticizing temperature. c) Rivet plastic deformation (forging phase) when the rivet stops rotating and the axial force increase, the plasticized metal rivet tip is pushed against the cold polymeric layer, creating a resistance to deform the metal. d) Joint consolidation: The joint is consolidated during the cooling of the materials and the pressure. In the end, the spindle retracts, leaving the rivet inside the polymer. Figure 3 represents the diagram obtained from the process monitoring, describing each parameter according to the time, and illustrating the phases during the process [12].

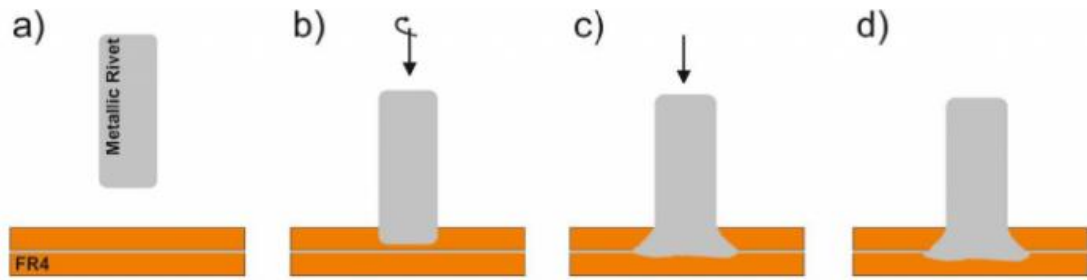


Figure 2: Schematic description of the Direct Friction Riveting process: a) positioning of joining partners, b) rivet insertion into the polymer (friction phase), c) rivet plastic deformation (forging phase), and d) joint consolidation [12].

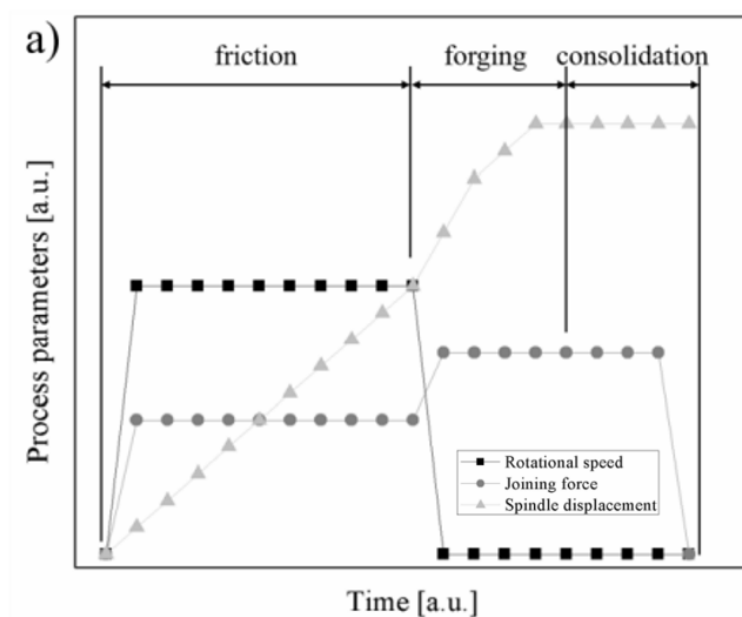


Figure 3: Schematic force-controlled FricRiveting diagram [12].

The Friction Riveting process can combine different types of controls culminating in different responses. For example, when the control is the joining force, the response will be the time and when the control is the time, the joining force is the

response. The friction riveting using force-controlled and time-limited is the most used in the research now a day [12].

2.1.2. Process Parameters

The five mainly controllable parameters for the friction riveting process for a conventional force-controlled and time-limited process with a forging phase are [12]:

1. Rotational Speed (RS): the speed of the spindle during the friction phase.
2. Frictional Time (FT): control the joining speed. It is the time between the spindle starts and stops rotating.
3. Frictional Force (FF): the axial force during the friction phase.
4. Forging Time (FoT): is the time for the forging phase.

In the force-controlled and displacement-limited process, the displacement at friction (DaF) is also a controllable parameter. Other parameters that can be analyzed are the consolidation force (CF), the consolidation time (CT), and the clamping pressure (CP).

2.1.3. Recent studies about friction riveting

The Friction Riveting Technique have been explored in many applications fields, such as in construction structures, aeronautics components, and the automotive industry. Blaga et.al. [2] demonstrated the feasibility of Friction Riveting on Glass fiber reinforced polyetherimide and titanium grade 2, which were selected as an alternative solution for truss girder connections in composite bridge construction.

The combination of polycarbonate (PC) and AA2024-T3 was explored in the application of the joints in the attachment of vehicle headlights [24]. The joints demonstrated good mechanical performance (between 6659 ± 62 N to 8540 ± 182 N - 68.4–87.8% of the ultimate tensile strength of the metallic rivet).

The first study reported in the literature using metal-thermoset composites joints explored the Ti-6Al-4V and pultruded glass fiber reinforced joint formation [25], showing composite degradation and, even so, the joints achieved good rivet penetration depth and widening of the rivet tip.

2.2 Joint Design Optimization

Design of experiments (DOE) is a statistical method widely used in industrial processes and research centers to select the optimal level settings for the control factor intending to optimize the production and improve the quality of the process, besides helping to understand the relationship between the variables and those influences on the final properties [13].

The Response Surface Methodology (RSM) is a statistical design optimization that is mainly used in processes where several independent variables influence some responses of the process. This method consists of exploring the space between the variables, aiming to find a relationship between them, and the best combination that optimizes the process [14]. This method improves the optimization by evaluating the effect of the one-variable-at-a-time [15].

Box-Behnken Design (BBD) is a type of DOE that fits the RSM using three levels ($3k$), and all factors should be adjusted by them. The main advantage of BBD compared with other three levels designs is the possibility of points selection from a three-level factorial arrangement, that there are no factorial or extreme points and requires few points. The number of experiments (N) for BBD is given by the equation, where k is the number of variables and C_o is the number of center points [15].

$$N = 2k(k - 1) + C_o \quad (1)$$

3. Materials and Methods

3.1. Materials

3.1.1. Aluminum Alloy 2024 - T351

The 2024 aluminum is a heat treatable alloy mainly composed of aluminum, copper, and magnesium (Table 1 shows the alloy composition). This alloy is widely used in the aeronautical industry and its main properties are good mechanical properties (325 MPa yield strength and 470 MPa tensile strength [16]), reasonable corrosion resistance, and good machinability.

Table 1 - AA 2024 chemical composition [16].

Element	Cu	Mg	Si	Fe	Mn	Cr	Zi	Ti	Al
% Weight	3.8-4.9	1.2-1.8	<0,5	0,5 max	0.3-0.9 max	0.1 max	0.25 max	0.15 max	.bal

The T351 indicates that this alloy went through a heat treatment, which consists of solubilization to achieve a supersaturated solution of copper in aluminum. After that, it is submitted to a hardening process followed by an aging process [9]. The melting point of this aluminum alloy is between 502°C (solidus) and 638°C (liquidus) [16]. Figure 4 illustrates the microstructure and microhardness of the rivet material. The microstructure is characterized by elongated grains due to the extrusion process. A homogeneous hardness distribution is present with values around 155 HV.

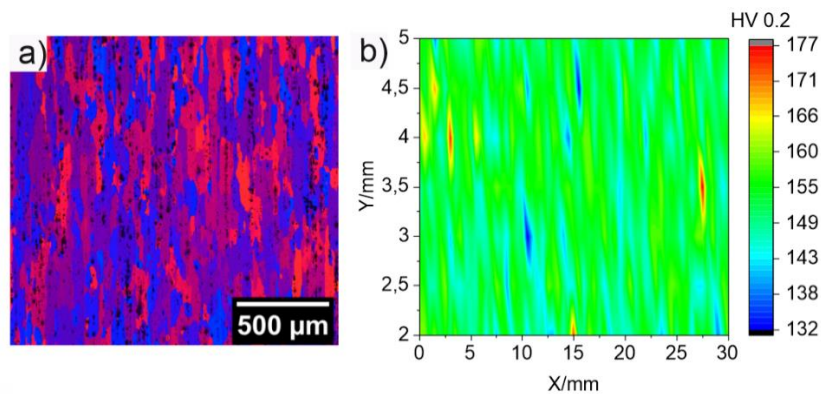


Figure 4: a) microstructure analysis and b) microhardness map of the AA 2024-T351 rivet in the extrusion direction.

AA2024-T351 rivets with 5 mm and 4 mm diameter and 60 mm and 40 mm length, respectively, were used (Figure 5). Once with a smaller diameter, the length has to be also smaller to reduce the warp chances.

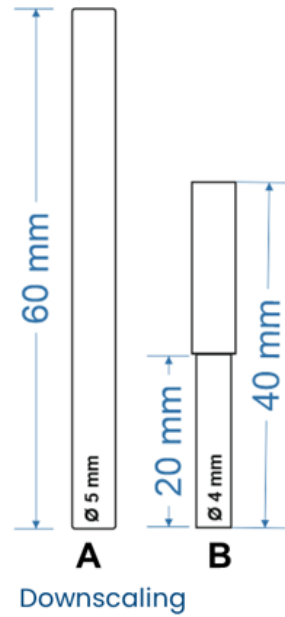


Figure 5: Illustration of the aluminum rivets: A) 5 mm and B) 4 mm diameter.

The rivet diameter on the side to be inserted in the joining equipment's spindle was kept constant for all tested rivet geometries.

3.1.2. Glass-Reinforced Epoxy Laminate Material (FR4)

Glass-reinforced epoxy resin laminates, the most used material for PCB confection, with a single copper layer on one side and a double copper layer adhered to either board side, were used to manufacture the joints. These PCBs materials are named FR4 by NEMA (National Electrical Manufacturers Association, USA), where 'FR' stands for flame retardant material [17]. The thickness of the used plates is 1.5 mm, which is among the highest of PCBs commercially produced. The FR4 glass fiber epoxy is the most popular and versatile material used in PCBs, mainly because of the good resistance-weight ratio and the capacity to maintain the high mechanical strength, and the good insulation in humid environments [18]. Figure 6 illustrates the FR4 microstructures used in this study, with double (Figure 6a) and single copper layer (Figure 6b), alongside the sketch of Cu-layer-FR4 distribution and the material thickness. Table 2 shows the physical-chemical properties of FR4 material.

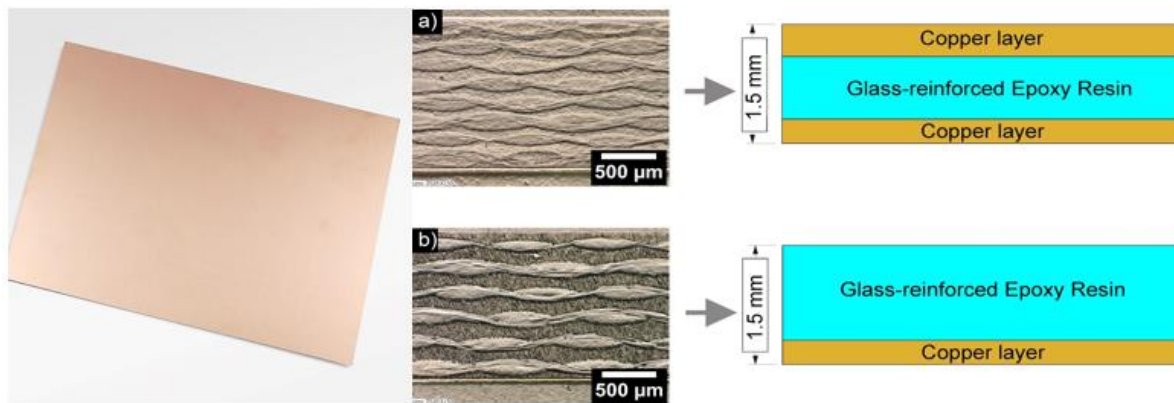


Figure 6: FR4 plate and cross-sectional microscopy view from a) plates with two copper layers and b) single copper layer.

Table 2 - Physical-chemical properties of FR4 material.

Glass Transition Temperature – Tg (°C)	124 ± 9
Degradation Temperature (°C)	328 ± 2

3.2. Methods

3.2.1. Joining Equipment and Procedure

The joints were produced at Hereon using the dedicated Friction Riveting laboratory equipment. A sample holder with a pneumatic clamping system (DZF-50-25-P-A-FESTO, Islandia, NY, USA) was used to fix the overlapped PEI and PCBs plates. This work adopted a direct-Friction Riveting process variant controlled by force and limited by spindle displacement [19]. Figure illustrates the FricRiveting laboratory equipment at Hereon (RNA – Reibnietanlage, germ.) developed in cooperation with Henry Loitz Robotik. The machine consists of a high-speed friction welding system RSM410 manufactured by Harms & Wende GmbH & Co. KG, which permits maximum spindle rotation of 21000 rpm and a maximum axial force of 24 kN and maximum torque of 20 Nm.



Figure 7: Automated RSM 410 welding system for the production of friction-riveted joints (image source: Hereon).

The joints were produced by varying three main parameters of this process: rotational speed (RS), displacement at friction (DaF), and joining force (JF). A one-factor-at-a-time (OFAT) approach was applied to obtain a combination of joining parameters until valid joints (deformed and anchored metallic rivets within the FR4-PCB plates) were obtained. Table 3 lists the selected joining conditions investigated in this work and characterized. The selected joining conditions for the 5 mm rivet show the significant difference in deformation and joint formation obtained by different plate stacking configurations and only minimal changes in displacement at friction (as a result of the reduced plate thickness). Condition 1 was applied to four FR4-PCB plates overlapping with double copper layers adhered to either side of the board. Condition 2 was used for two FR4-PCB plates overlapping with a single copper layer adhered to one side (lower side). It has to be noted that the work intended to produce overlapped joints of two plates. The additional two plates were intended to avoid welding the rivet to the equipment's

working table in case of full perforation. Aiming to analyze the joint formation with the 4mm diameter rivet, the parameters used for condition 2 was considered in the first trial. Table 3 shows the parameters range used for these mentioned trials. The material variation is described by I Cu and II Cu, which means that was used the FR4 material with one copper layer and two copper layers, respectively.

Table 3 - Joints parameters for the first trials.

Conditions	Layer number	Rivet Diameter	Rotational Speed (RS)	Displacement (DaF)	Joining Force (JF)
C1	II Cu	5 mm	7000 rpm	3.5 mm	4000 N
C2	I Cu	5 mm	7000 rpm	3.0 mm	4000 N
C3	I Cu	4 mm	7000 rpm	3.0 mm	4000 N
C4	I Cu	4 mm	6000 rpm	3.0 mm	4000 N
C5	I Cu	4 mm	5500 rpm	3.0 mm	4000 N

After the one-factor-at-time approach, the process parameters were optimized using the Box-Behnken response surface design method (BBD).

Table 4 summarizes the parameters windows investigated for the FR4 plates, with a single and double copper layer, with a 4 mm rivet diameter.

Table 4 - Design of Experiments (Box-Behnken surface designer) for the joints with 4 mm rivet. RS: rotational speed; DaF: displacement at friction; JF: joining force.

Sample	RS [rpm]	DaF [mm/100]	JF [N]	Material
1	3000	300	3000	II Cu
2	5000	300	3000	I Cu
3	3000	300	3000	I Cu
4	7000	240	3000	II Cu
5	3000	270	4000	I Cu
6	7000	270	3000	I Cu
7	5000	240	4000	II Cu
8	5000	300	4000	II Cu
9	5000	240	4000	I Cu
10	5000	300	4000	I Cu
11	3000	270	4000	II Cu
12	7000	270	4000	II Cu
13	5000	240	2000	I Cu
14	3000	240	3000	II Cu
15	7000	270	2000	I Cu
16	3000	270	2000	I Cu
17	7000	270	2000	II Cu
18	5000	240	2000	II Cu
19	5000	270	3000	I Cu
20	5000	270	3000	I Cu
21	7000	300	3000	II Cu
22	7000	270	4000	I Cu
23	7000	240	3000	I Cu
24	3000	240	3000	I Cu

25	5000	300	2000	II Cu
26	5000	270	3000	II Cu
27	5000	270	3000	II Cu
28	3000	270	2000	II Cu
29	5000	270	3000	II Cu
30	5000	300	2000	I Cu

3.2.2. Process Temperature Evolution, Microstructure, and Local Mechanical Properties

During the joining process, the temperature evolution was recorded on the softened material expelled as a flash outside the joint region using an infrared camera (Image IR8800, InfraTec, Germany), a filter gap of 150°C-700°C was selected. The results processed with the IRBIS 3 software were associated with the revealed joint microstructures evaluated through optical microscopy (LOM).

3.2.3. Joint Formation Analysis

The joints produced with AA2024 rivets with PEI, FR4, and PCB-FR4 were assessed by optical microscopy (LOM, Keyence VHX-6000, and Leica). For this procedure, the samples were prepared following standard metallography procedures. The width (W) of the deformed rivet tip and its insertion depth (H), and the anchoring depth (DP) were measured within the FR4 laminate, using the cross-section images generated from LOM. W, H, and DP values were used to evaluate the rivet anchoring efficiency by calculating the volumetric ratio (VR) (Equation 1). This formulation was developed in previous studies with FricRiveting [19] and describes the rivet anchoring considering the interaction volume between plastic material over the deformed rivet.

$$VR = \frac{Dp \cdot (W^2 - D^2)}{H \cdot W^2} \quad (1)$$

3.2.4. Local and Global Mechanical Performance

Local mechanical properties were evaluated by Vickers microhardness testing equipment, following ASTM E384-992e1 [20]. The global mechanical performance of the joints was analyzed through ultimate tensile force (UTF), using a universal testing machine (Zwick Roell 1484, Germany) equipped with a 100 kN load cell. Tests were performed at room temperature at a traverse speed of 1 mm/min, in type “T” spot joint configuration, with 40 mm grip distance. This configuration uses a specially designed specimen holder, as shown in Figure 8 [21]. The samples fractured during the test were photographed for analysis of fracture modes and their fractured surfaces were analyzed by digital microscope (VHX-6000series from KEYENCE America) and scanning electron microscope (Quanta FEG 650).

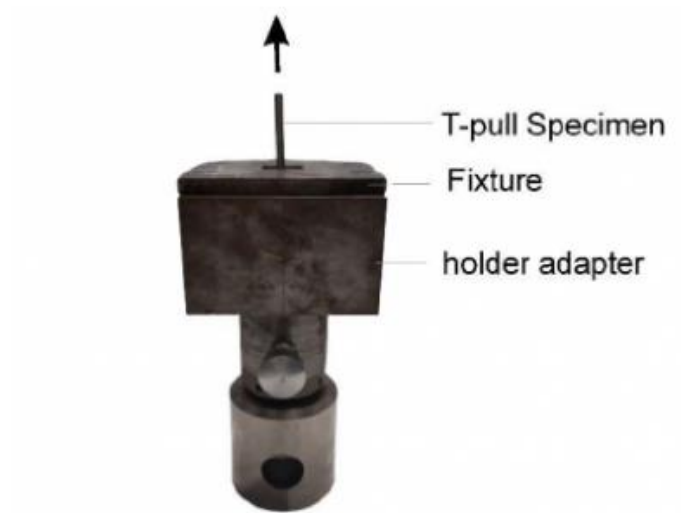


Figura 8: T-pull tensile testing holder adapter used to evaluate the tensile force properties in Friction Riveting.

4 Results and Discussion

4.1. 5 mm rivet diameter

4.1.1. Joint Formation

Figure 9 presents examples of the joints' anchoring zones within the mid-cross sections for the two investigated parameter sets and material configurations. Three replicates were produced for each condition. The resulting geometrical properties, which characterize the joint formation, are summarized in Table 5. Figure 9 shows a representative joint geometry for Condition 1 (AA-2024-T3 rivet and FR4-PCB double copper layer), where the generated frictional heat resulted in the drilling of the rivet through the four FR4-PCB laminates. The metallic rivet achieved 5.5 ± 0.1 mm of penetration depth into successive FR4-PCB plates without generating sizeable deformation of the rivet tip ($W = 4.8 \pm 0.3$ mm, the width of initial rivet diameter before the joining) and anchoring depth ($DP = 0$ mm), resulting in a joint with no volumetric ratio and the perforation of successive FR4 plates, therefore a not successful Friction Riveting joint. Many improved joints were achieved for Condition 2 (AA-2024-T3 rivet and FR4-PCB single copper layer); see Figure 9b. The slight change in DaF for Condition 2 aimed to reduce the rivet insertion depth to avoid successive penetration of multiple plates. Additionally, it is intended to verify if the heat generated is sufficient to produce significant deformation of the rivet tip into FR4-PCB with fewer copper layers. The combination of parameters and material configuration achieved heat generation levels sufficient for effective anchoring of the rivet into two FR4-PCB overlapped laminates without perforation of more than two plates. The gap between the two overlapped FR4 plates was caused by the large deformation (from 5.0 mm to 8.7 ± 0.8 mm). The joints obtained show 2.3 ± 0.1 mm penetration, 1.7 ± 0.1 mm anchoring depth, and 8.7 ± 0.8 mm width deformation. A significant volumetric ratio ($VR = 0.50 \pm 0.02$) was achieved at anchoring depths below 3.0 mm, the lowest thickness achieved with the Friction Riveting process so far.

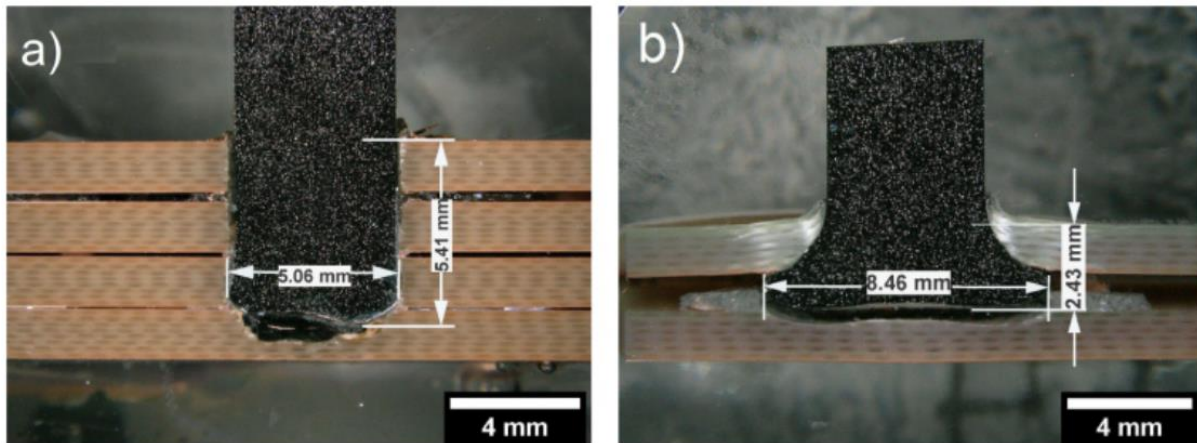


Figure 9: OM micrographs of joint cross-sections produced with the joining conditions 1 and 2. *H*-values are related to the penetration depth and *W*-values to the deformation rivet tip of a) Condition1 (unsuccessful) and b) Condition 2 (successful joint condition).

Table 5 - Geometrical features (*W*, *H*, and *DP*) of the friction-riveted joints and calculated volumetric ratio, *VR*.

Joining Condition	<i>H</i> [mm]	<i>W</i> [mm]	<i>D_p</i> [mm]	<i>VR</i> [a.u]
Condition 1				
(double copper layer) (RS-7000 rpm; FF-4000 N; DaF-3.5 mm)	5.5 ± 0.1	4.8 ± 0.3	-	-
Condition 2				
(one single copper layer) (RS-7000 rpm; FF-4000 N; DaF-3.0 mm)	2.3 ± 0.1	8.7 ± 0.8	1.7 ± 0.1	0.50 ± 0.02

The different joint formations achieved might also be related to the strong anisotropic character of the FR4-PCBs material due to the significant difference between copper and glass-epoxy thermal properties [22]. The placement of a single or double-layer in the board significantly influences the generated heat during the Friction Riveting

process, as the process starts with initial Coulomb friction and subsequent changes in material viscosity during the rivet insertion.

4.1.2. Temperature evolution

Figure 10 shows the process temperature measurements via infrared thermography (Figure 10a) and the average peak temperatures (Figure 10b) recorded on expelled flash material from three joint replicates manufactured with Condition 2. From the temperature measurement, the average temperature obtained from three joint replicates manufactured with Condition 2 was 362 ± 7 °C, which is approximately 70% of the rivet melting temperature. The temperature achieved shows that the generated heat is sufficient to promote the rivet deformation despite the minimal material thickness. Besides that, through this analysis, it is possible to conclude that the composite was degraded once the temperature achieved was 10% higher than the degradation temperature for this material.

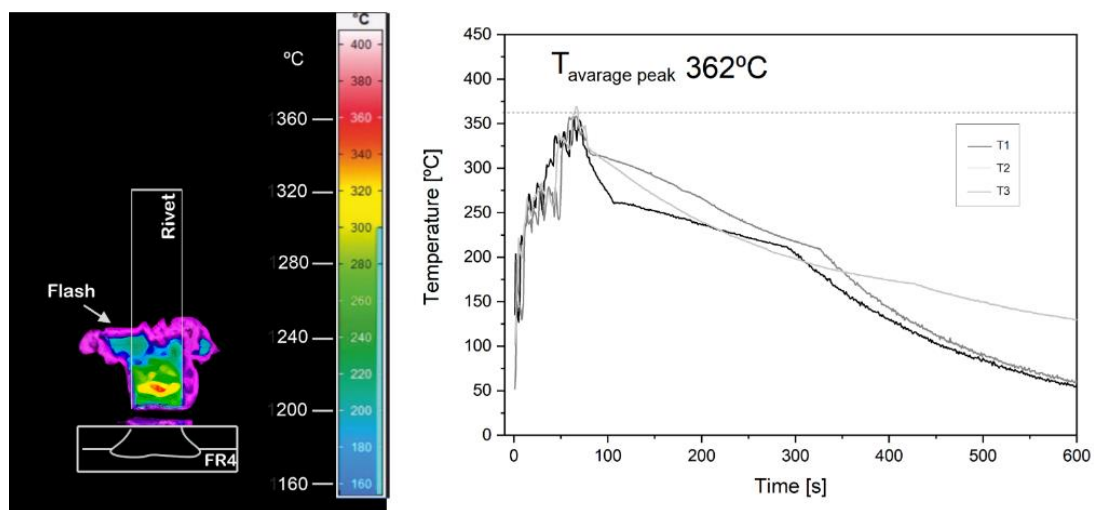


Figure 10: a) Infrared thermography of the process temperature development during Friction Riveting. b) Maximum average temperature (362 ± 7 °C) measured on the expelled thermoset flash material from three joints produced for Condition 2.

4.1.3. Microstructural Analysis and Local Mechanical Performance

Figure 11a shows the microstructure and the Vickers microhardness distribution of an AA-2024-T351 deformed rivet from the joining condition 2. Different

microstructural zones have been identified. In the thermo-mechanically affected zone of the metal (TMAZ) (Figure 11b), a realignment of grains was observed in the direction of the flow of forged and plasticized volumes. Partial grain refinement was also observed, characteristic of dynamic recrystallization in aluminum alloys, as reported for the PC-AA 2024-T351 joint [4] and another friction-based welding process [21]. In the heat-affected zone of the metal (HAZ) (Figure 11c), it is not possible to observe microstructural changes, compared with the base material (Figure 4), such as grain size variations.

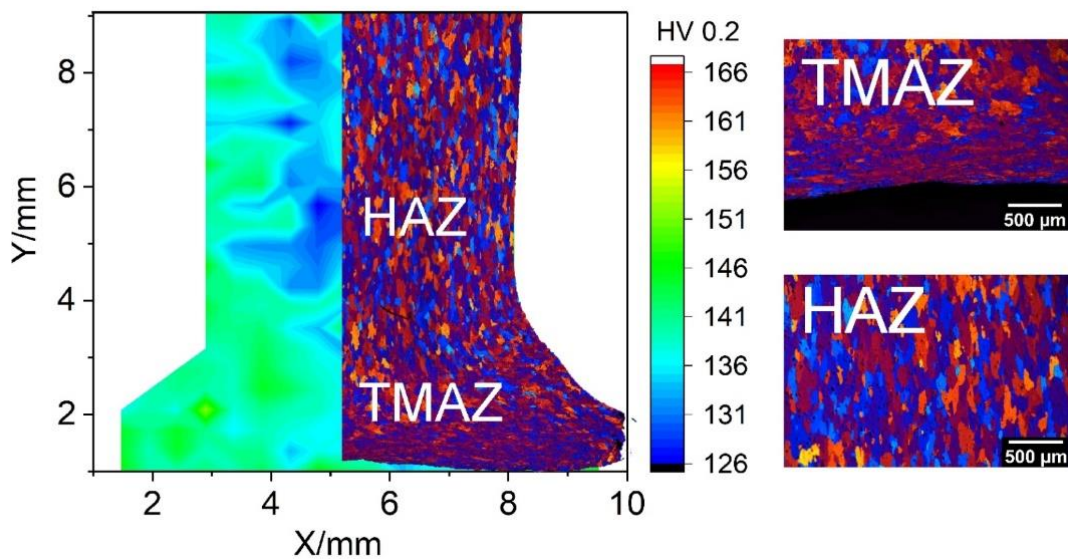


Figure 11: a) Microstructure features of a Friction-riveted PCB-FR4 single copper layer/AA-2024-T351 joint (Condition 2) and Vickers microhardness distribution of an AA 2024-T3 deformed rivet. b) Thermo-Mechanically Affected Zone of the metal, TMAZ, exhibits grain realignment in the direction of the material flow in the forged rivet tip c) Detail of the Heat Affected Zone of the metal, HAZ.

4.1.4. Global Mechanical Performance

Tensile tests were carried out to determine the strength of the successfully anchored joints obtained in Figure 12a. The average maximum tensile force of the two tested compounds was $828\text{N} \pm 65\text{N}$ and the failure modes resulting for these samples were due to delamination of the FR4 plates (Figure 12d).

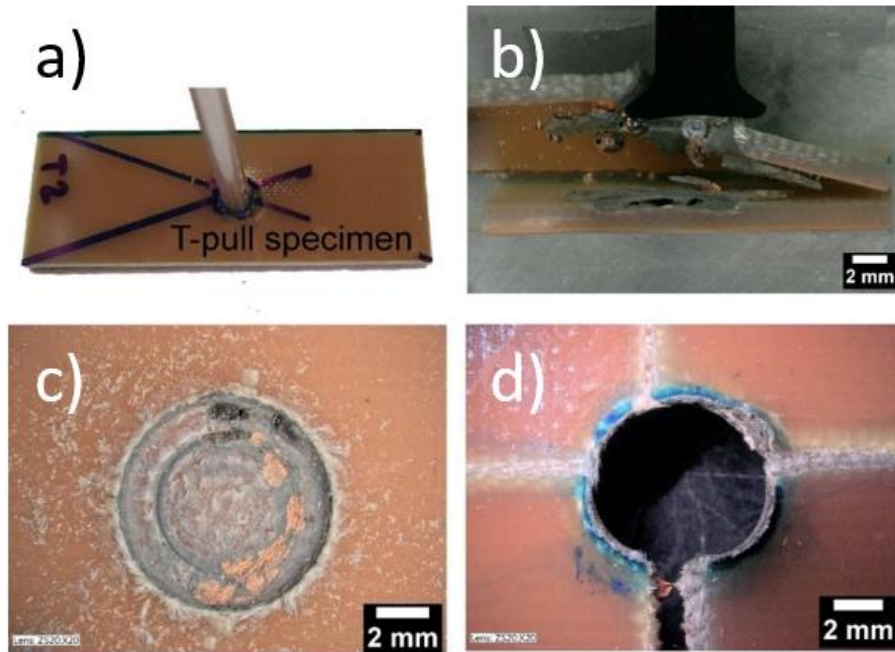


Figure 12: a) T-pull specimen before testing, b) cross-sectional view of failure through PCB plate, (c) lower and (d) upper FR4-PCB parts after T-pull testing.

The tensile force achieved is considered moderate compared with other studies [23], which achieved 1,9 kN – 4,0 kN on a tensile test to glass-fiber-reinforced polyetherimide composite and titanium grade 2 hybrid joints.

4.2. 4 mm rivet diameter

4.2.1. Joint formation

As already mentioned in section 3.2.1. Joining Equipment and Procedure, the first trial was accomplished with the same parameters, which led to a successful anchored joint with a 5 mm rivet. It is possible to see in Figure 13a that using a 4 mm rivet. The rivet was successfully anchored but with large penetration once the goal is achieved with less than 3 mm insertion. This result was achieved due to the higher pressure applied to the plate once the contact area is smaller and the force is the same. Thus, the rotational speed was reduced for the next trial (Condition 4), leading to a better result and similar to condition 2, as shown in Figure 13b. Decreasing, even more, the rotational speed (Condition 5), the result was a joint with good deformation, but the anchoring is impaired by the metal going through the upper surface of the composite plate, as shown in Figure

13c. In Table 6 the geometrical feature for these trials is compiled, including the calculated volumetric ratio (VR).

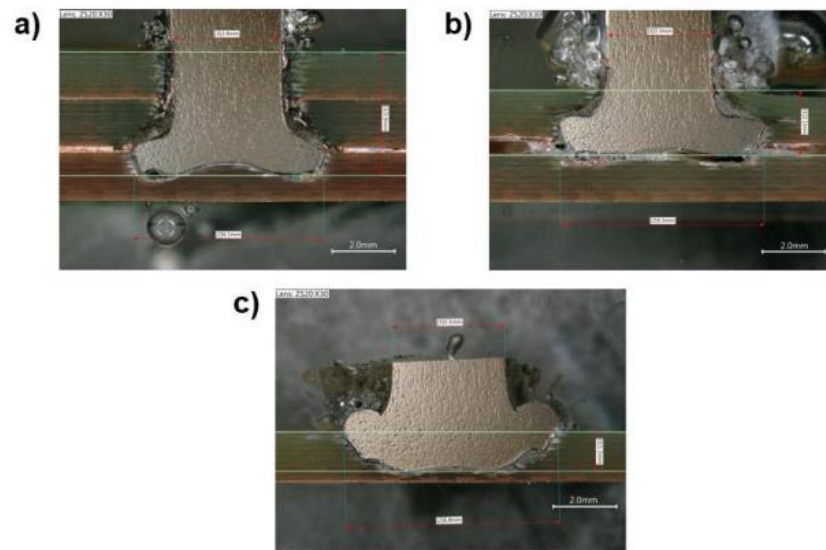


Figura 13: Trials for 4mm rivet and FR4 joint – a) C3 (RS-7000 rpm; FF-4000 N; DaF-3 mm); b) C4 (RS-6000 rpm; FF-4000 N; DaF-3 mm); c) C5 (RS-5500 rpm; FF-4000 N; DaF-3 mm).

Table 6 - Geometrical features (W, H, and DP) of the friction-riveted joints and calculated volumetric ratio, VR.

Joining Condition	H [mm]	W[mm]	D _p [mm]	VR [a.u]
One copper layer				
C3				
(RS-7000 rpm; FF-4000 N; DaF-3 mm)	3.9	6.1	3	0.53
C4				
(RS-6000 rpm; FF-4000 N; DaF-3 mm)	2.1	6.5	1.6	0.56
C5				
(RS-5500 rpm; FF-4000 N; DaF-3 mm)	1.2	6.8	-	

Intending to reach the best combination of parameters, starting from these three first trials results, the rotation speed (RS), the joining force (JF), the displacement (DaF) as well as the number of copper layers were combined for a DOE, which will be described in the next section.

4.2.2. Determination of process-properties-performance correlations and optimization approach via DOE

The Box-Behnken Design generated 30 conditions, as already mentioned in section 3.2.1. From these conditions, samples were produced and the process temperature and the ultimate tensile force were measured. Table 7 shows the values obtained by temperature measurement and T-pull test for the DOE joints numbered from 1 to 30 shown in section 3.2.1 in the Box-Behnken surface design in Table 4. From these conditions, mathematical models were obtained to statistically analyze the significance of each parameter and its interaction with the responses.

Table 7 - Tensile and temperature response from the DOE analysis.

Conditions	UTF [N]	Temperature [°C]
1	77	327
2	10	403
3	501	243
4	911	270
5	751	289
6	29	387
7	0	386
8	937	300
9	7	331
10	14	366
11	63	351
12	30	399
13	768	330
14	87	318
15	32	490
16	57	230
17	0	438
18	0	383
19	678	312
20	718	293
21	8	403
22	0	399

23	1	385
24	746	266
25	21	424
26	0	387
27	5	370
28	17	273
29	0	416
30	828	284

4.2.3. Effect of the Temperature

Regarding the temperature, it can be seen in Figure 14 that the rotational speed (A) and the combination with the material (AB) are the most influents ones. The higher rotational speed contributes to greater friction between the metal and the composite. Besides that, the high conductivity of the copper contributes to the heating spread. Comparing the joints C1 and C3, which were both processed with 3000 rpm rotational speed (the lowest analyzed), 300 mm spindle displacement, and 3000 N joining force, but with different materials (II Cu and I Cu, respectively), is possible to observe an increase of 35% in the temperature when one more copper layer is added. However, comparing the joints C2 and C21 with the highest rotation speed analyzed, the temperature does not change. In this regard, the copper layer's influence on the temperature is noticed when the rotation speed is at the lowest level.

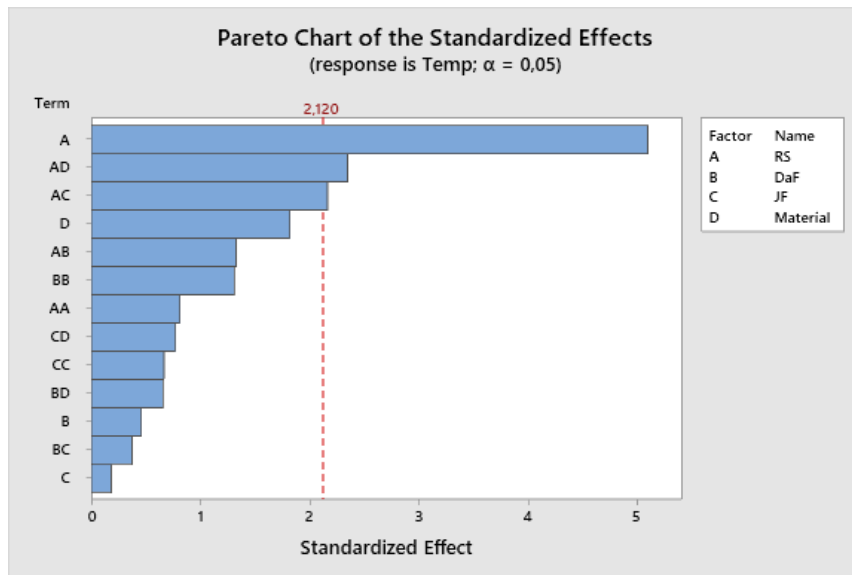


Figure 14: Pareto Chart obtained with temperature response from the combination of the parameters: rotational speed (parameter A), displacement of the spindle (parameter B), joining force (parameter C), and the material (parameter D).

The interaction between the joining force (JF) and the rotational speed (RS) is the most influential one discarding the material variation. Fixing the displacement on 2.7 mm (the intermediate level) and the material with 1 copper layer, the surface plot Figure 15a, and the contour plot Figure 15b were obtained for temperature with rotation speed and joining the force. It is possible to see that the joining force culminates in a small temperature increase. A high JF and high RS combination generate a high process temperature, between 400°C - and 450°C. However, a low JF with a high RS is enough to make the process achieve the maximum temperature.

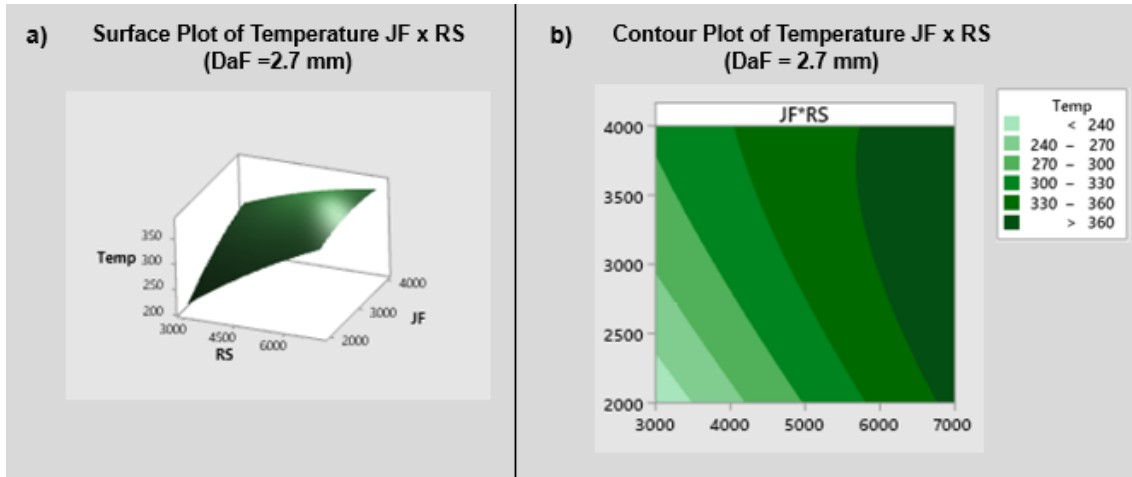


Figure 15: (a) Surface plot and (b) contour plot of temperature in function of joining force (JF) and rotational speed (RS).

In Figure 16, it is possible to compare the contour plot between all parameters combinations. From the contour plot with DaF x RS (Figure 16a), it is possible to observe that the temperature varies just with RS, keeping almost constant with DaF. From the contour plot with JF x DaF (Figure 16c), it is possible to observe that by increasing the DaF value with JF constant value in a range of 2000N-2300N, the temperature decreases. From this, it can be inferred that the DaF, in this case, is not related to the friction between the joint materials, and this behavior is a consequence of the contribution of other factors in the quantitative analysis. When the JF is high enough (higher than 3000N), the temperature achieves its higher value on the scale and the influence of DaF is no longer significant.

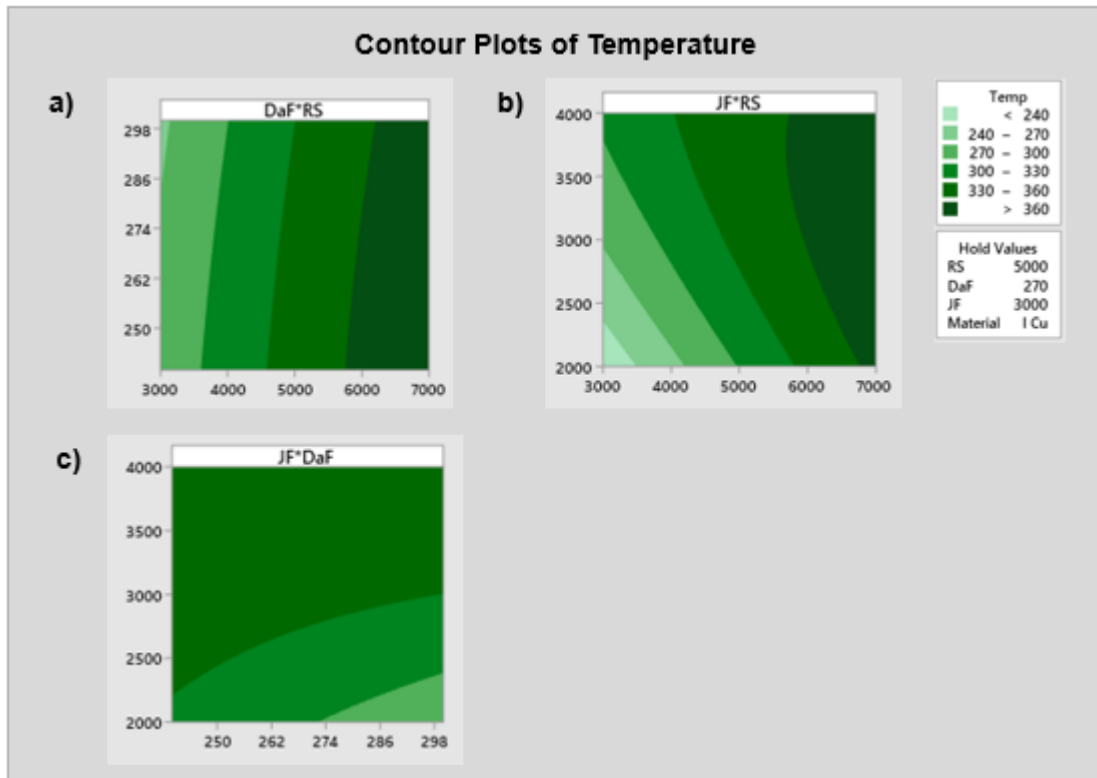


Figure 16: Contour plot of temperature for the parameters combination: a) DaF x RS, b) JF x RS and c) JF x DaF.

4.2.4. Effect of the Global Mechanical Properties

Figure 17 shows that the standardized effect significant is higher than the standardized effect of all factors and interactions. This is explained by the instability of the mechanical performance of the joints and the test deviation. Once the plates have a small amount of the plate material to deform, a slight difference between the width and the insertion of the deformed rivet tip can generate considerable divergence between the UTF values. The samples with 0N until 100N are unstable, considering that even a low pressure applied during the clamping can interfere with this value once the failure, as shown in section 3.2.4., occurs through delamination layer by layer. Besides that, the thermoset degrades before plasticizing, generating pores within the joint, as shown in section 4.2.1. These pores interfere in mechanical performance and are a not controllable response. Borba [12] found the same volumetric defects while working with thermoplastic composites due to severe plastic deformation and induced thermal degradation.

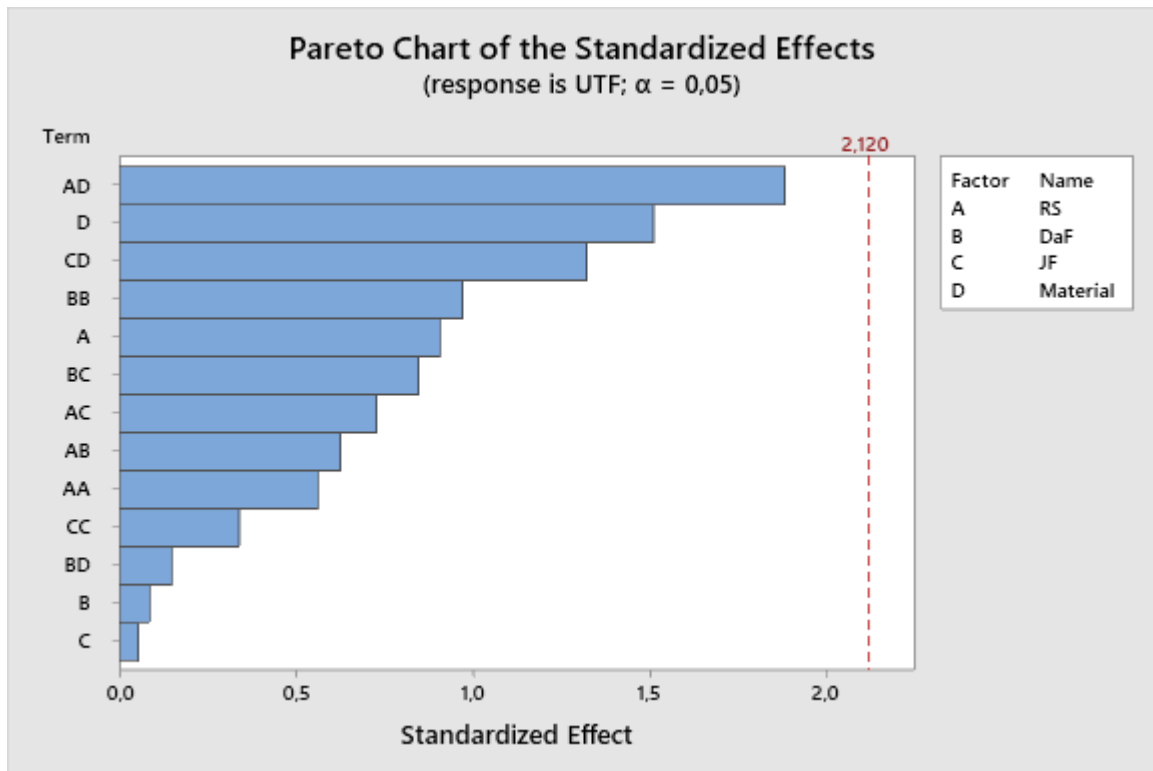


Figure 17: DOE graph with a surface response showing the influence on the ultimate tensile force (UTF) of each parameter analyzed and their combination.

The most influential interaction is also the material with the rotational speed (RS). Relating to the temperature analysis is possible to identify that the mechanical behavior is also associated with the degradation rate of the material. A higher RS generates a higher heating input, which degrades the thermoset, leading to a low plate resistance.

The displacement influence the high of the deformation insertion, which interferes with the joining force in different ways once this insertion should be sufficient deeper to achieve two plates or deeper enough to make the joint in the middle of the first plate and not so close to the surface to generate good mechanical performance.

6. Conclusions

This study demonstrated the feasibility of using the Friction Riveting process as an alternative to the Press-Fit fasteners process in printed circuit boards (PCB) manufacture.

With the anchorages of AA2024 in FR4, printed circuit boards with 5 mm rivet and single and double copper layers were possible to obtain good deformation with anchoring, with 60% of the rivet tip deformed at 2.43 mm penetration depth in the FR4 laminate. The joints present significant anchoring efficiency (volumetric ratio $VR = 0.50 \pm 0.02$), achieved at thicknesses and anchoring depths below 3.0 mm, which is considered the lowest depth achieved with Friction Riveting so far. The heating and the applied process forces resulted in microstructural changes and reduction of local mechanical properties, with grain refinement and realignment within the deformed rivet tip. The joints' mechanical performance was evaluated in terms of ultimate tensile force, reaching $828 \text{ N} \pm 65 \text{ N}$, with failure occurring through FR4-PCB due to plate bending, followed by delamination.

From the DOE studies of the 4 mm rivet diameter joints, it is possible to conclude that the rotational speed is the most influential variable in the process. Considering the effect on the temperature generated during the process, this variable alone shows a high impact, followed by the combination with the material (one or double copper layer), once the higher rotational speed generates greater friction between the metal and the composite and the high conductivity of the copper contributes to the heating spread.

7. REFERENCES

- [1] AMANCIO FILHO, S. T.; BEYER, M.; DOS SANTOS, J. F. Method of connecting a metallic bolt to a plastic workpiece. US 7575149 B2, 2009.
- [2] BLAGA L., AMANCIO FILHO S. T., DOS SANTOS J. F., BANCILA R. Friction riveting of civil engineering composite laminates for bridge construction, ANTEC 2012, 1-4 April, Orlando-Florida, 2012
- [3] MALLMANN, P.H.S., BLAGA, L., AMANCIO FILHO S. T., DOS SANTOS J. F. FRICTION RIVETING OF 3D PRINTED POLYAMIDE 6 WITH AA 6065-T6. Procedia Manufacturing. 23rd International Conference on Material Forming (ESAFORM 2020), 2020.
- [4] Rodrigues, C. F. REBITAGEM POR FRICÇÃO DE ALUMÍNIO 2024-T351 EM POLICARBONATO. Thesis (Engineering Doctorate), Universidade Federal de São Carlos, São Carlos – SP, Brasil, 2014.
- [5] Blaga, L.A Bancila, R. Santos, J.F. and Amancio-Filho, S.T. Friction Riveting of glass-fiber-reinf polyetherimide composite and titanium grade 2 hybrid joints. Materials and Design, 2013, 50:825–829.
- [7] Altmeyer, J., dos Santos, J.F., Amancio-Filho, S.T. Effect of the Friction Riveting process parameters on the joint formation and performance of Ti alloy/shortfiberforced reinforced polyether ether ketone joints. Materials Designer 60:164– 176, 2014.
- [8] Proenca, B. Blaga, L.A.Santos, J.F. Canto, L.B. Amancio-Filho, S.T. Force controlled friction riveting of glass fiber reinforced polyamide 6 and aluminum alloy 6056 hybrid joints. In Proceedings of the Annual Technical Conference- ANTEC, 2015
- [9] Borba, N. Z. Afonso, C. Blaga, L. A. et al. On the Process-Related Rivet Microstructural Evolution, Material Flow and Mechanical Properties of Ti 6Al4V/GFRP Friction-Riveted Joints. Materials (Basel), 2017, 10:184. DOI/10.3390/MA10020184
- [10] Würth Elektronik 2017, Press-Fit Technology, Würth Elektronik, viewed 9th September 2021, https://www.weonline.com/web/en/electronic_components/news_pbs/blog_pbcm/blog_detail-worldofelectronics_65278.php

[11] Multi CB, Printed Circuit Boards, Press-Fit Technology, Multi CB, viewed 9th September 2021, < <https://www.multi-circuit-boards.eu/en/pcb-design-aid/drills-throughplating/press-fit-technology.html>

[12] Zocoller Borba, N.: Design and mechanical integrity of friction riveted joints of thermoplastic composite. Thesis (Engineering Doctorate), Technischen Universität Hamburg, Germany, 2020. (DOI: /10.15480/882.2959).

[13] BOOKER J.D., 2003, Industrial practice in designing for quality. International Journal of Quality Reliability and Management, v. 20, n. 3, p. 388-203.

[14] Kathleen M. Carley, Natalia Y. Kamneva, Jeff Reminga, Response Surface Methodology. CASOS Technical Report. Carnegie Mellon University, School of Computer Science, Pittsburgh, 2004.

[15] Florentinus Dika Octa Riswanto, Abdul Rohman, Suwidjiyo Pramono, Sudibyo Martono, Application of response surface methodology as mathematical and statistical tools in natural product research. Journal of Applied Pharmaceutical Science (JAPS). Cross Mark, Volume 9, October 2019.

[16] ASM INTERNACIONAL. Metals Handbook vol.2: Properties and selection – nonferrous alloys and special-purpose materials. Materials Park, OH: ASM Internacional, 1990.

[17] <https://www.proto-electronics.com/blog/the-4-electronic-componentsuppliers-of-proto-electronics-0>. Acces: 18/08/2021.

[18] <http://www.nanotech-elektronik.pl/index.php/en/info/materials>. Acces: 18/08/2021.

[19] Cipriano, P. G. Ahiya, A. dos Santos, J.F. Single-phase Friction Riveting: metallic rivet deformation, temperature evolution, and joint mechanical performance. Weld World, 64: 47–58, 2020. DOI 10.1007/S40194-019-00803-3.

[20] ASTM E384-992e1: Test Method for Microindentation Hardness of Material, ASTM International, USA, 2005.

[21] Amancio-Filho, S.T Blaga, L.A. Joining of polymer-metal hybrid structures: principles and applications. John Wiley & Sons, Inc, Hoboken, NJ, 2018.

[22] Andonova, A. Kafadarova, N. Pavlov, G. Investigation of thermal conductivity of PCB. Electronics, 2006. DOI10.1109/ISSE.2009.5207019

[23] BLAGA, L., Bancila, R., AMANCIO FILHO S. T., DOS SANTOS J. F. Friction Riveting of glass-fiber-reinforced polyetherimide composite and titanium grade 2 hybrid joints. Elsevier. Materials and Design 50 (2013) 825–829, 2013

[24] C. F. Rodrigues, L. A. Blaga, J. F. dos Santos, L. B. Canto, E. Hage Jr., e S. T. Amancio-Filho, “FricRiveting of aluminum 2024-T351 and polycarbonate: Temperature evolution, microstructure and mechanical performance”, J. Mater. Process. Technol., vol. 214, no 10, p. 2029–2039, Out. 2014.

[25] Zocoller Borba, N.: Friction Riveting of TI-6AL-4V and Pultruded Glass Fiber Reinforced Thermoset Polyester Hybrid Joints. Master Thesis (Material Science and Engineering). Federal University of São Carlos, São Carlos, 2015.